Article

A Simple and Regulable DNA Dimer Nanodevice to Arrange Cascade Enzymes for Sensitive Electrochemical Biosensing

Ding Wang, Ya-qin Chai, Yali Yuan, and Ruo Yuan

Anal. Chem., **Just Accepted Manuscript** • DOI: 10.1021/acs.analchem.0c03396 • Publication Date (Web): 17 Sep 2020

A Simple and Regulable DNA Dimer Nanodevice to Arrange Cascade Enzymes for Sensitive Electrochemical Biosensing

Ding Wang, Yaqin Chai, Yali Yuan*, Ruo Yuan*

Key Laboratory of Luminescence Analysis and Molecular Sensing (Southwest University), Ministry of Education, College of Chemistry and Chemical Engineering, Southwest University, Chongqing 400715, P. R. China

* Corresponding author. Tel.: +86-23-68252277; Fax: +86-23-68253172.

E-mail address: y198688@swu.edu.cn (Y. L. Yuan); yuanruo@swu.edu.cn (R. Yuan)

Abstract

Herein, a simple and regulable DNA dimer nanodevice was obtained by the assembly of two hairpin DNA monomers of H1 and H2 to control the distance between model enzymes HRP and GOx for sensitive electrochemical detection of microRNA. In detail, auto-terminated DNA polymerization reaction was designed on H1 and H2 monomers that decorated with HRP and GOx, respectively, to produce two half-released DNA monomers, which were spontaneously hybridized to each other, thereby obtaining a DNA dimer nanodevice with rigid dsDNA linker between two DNA monomers. By varying the length of dsDNA linker on DNA dimer nanodevice, the distance between GOx and HRP had been regulated to the optimum and the most efficient enzyme cascade reaction was acquired for constructing sensitive electrochemical microRNA-21 biosensor with a detection limit of 0.03 pM. In summary, the proposed DNA dimer nanodevice avoided the disadvantages of poor biocompatibility and controllability originated from traditional scleroid scaffolds, meanwhile showed obvious advantages in terms of assembly yield than previous complicated DNA scaffolds, which provided a novel strategy for developing high-efficiency enzyme cascade catalytic system and showed great potential in other clinical diagnosis and bioanalysis application.

Introduction

In the living systems, highly efficient enzyme cascade reactions play an important role in signal amplification and conversion,[1,2] metabolism and propagation,[3,4] where their reaction efficiency is related to the regulation of interenzyme distance.[5-8] Here, favorable distance between cascade enzymes could facilitate the diffusion of cascade intermediates from one enzyme to another, leading to the enhancement of enzyme cascade catalytic efficiency.[9-11] Currently, different artificial scaffolds have been developed to regulate the interenzyme distance and applied in various biotechnology fields, including biosynthesis,[12,13] disease diagnosis,[14,15] and bioanalysis[16,17]. Traditional scleroid scaffolds[18-20] have been designed, but they encountered inevitable shortcomings of poor biocompatibility and controllability. Nowadays, DNA nanostructures have emerged as potential scaffolds to control interenzyme distance with nanoscale precision for their structural programmability and accurate addressability[21-24]. Varied DNA scaffolds including DNA origamis,[25-27], tetrahedron[28], triangular prisms[29] and tweezers[30,31] have been applied to locate cascade enzymes at predesigned positions and regulate highly efficient enzyme cascade reaction. However, their further application is still limited due to the intrinsic defect of complicated DNA nanostructures with low assembly efficiency and complex assembly procedure. Therefore, searching for a simple, efficient strategy to control interenzyme distance for high enzyme cascade catalytic efficiency is still an urgent task.

To solve this problem, in the present work, a simple DNA dimer nanodevice was assembled to regulate the interenzyme distance for high efficient enzyme cascade catalysis. In detail, auto-terminated DNA polymerization reaction was performed on two hairpin DNA monomers of H1 and H2 that decorated with HRP and GOx, respectively, to produce two half-released DNA

monomers. Afterwards, two half-released DNA monomers were spontaneously hybridized to each other, thereby obtaining a DNA dimer nanodevice with rigid dsDNA linker between two DNA monomers. Using the dsDNA linker as spacer, the distance between GOx and HRP could be systematically regulated by varying the spacer length on DNA dimer nanodevice and the optimal enzyme cascade catalysis was obtained. In comparison with other scaffolds, the proposed DNA dimer nanodevice prepared *via* the assembly of two simple DNA monomers not only avoided the disadvantages of poor biocompatibility and controllability originated from previous scleroid scaffolds, but also show obvious advantages in terms of assembly yield than previous complicated DNA scaffolds. As a proof of concept, a sensitive biosensor was constructed by utilizing the novel DNA dimer nanodevice to manipulate highly efficient enzyme cascade reaction.

As exhibited in Scheme 1, two isolated hairpin DNA monomers (H1 and H2) served as templates were ingenious designed for DNA polymerization reaction, and they were divided into two regions, including the primer-triggered chain growth region (poly A/T base sequences) and the terminated region (poly G/C sequences). Target microRNA-21 and assisted DNA (S1) were used as primers to hybridize with H1 and H2 monomer, respectively, which could induce chain growth reactions along the poly A/T sequence until they encountered poly G/C sequence. This was because that only dATP and dTTP provided energy in these polymerization reaction systems, thus poly G/C base sequence could shoulder the function of automatic block spacer to terminate DNA polymerization reaction. Finally, two half-released DNA monomers (H1 and H2) induced the assembly of an DNA dimer nanodevice on modified electrode surface to control the optimal distance between GOx and HRP, and a satisfactory enzyme cascade electrocatalytic signal was monitored than free cascade enzyme system, which could realize the sensitive detection for target

microRNA-21. In summary, this work developed a novel and simple DNA dimer nanodevice to arrange cascade enzymes on the nanoscale for high enzyme cascade catalytic efficiency, which paved an avenue for arrange other biomolecules system with ultimate biological analysis and assay applications.

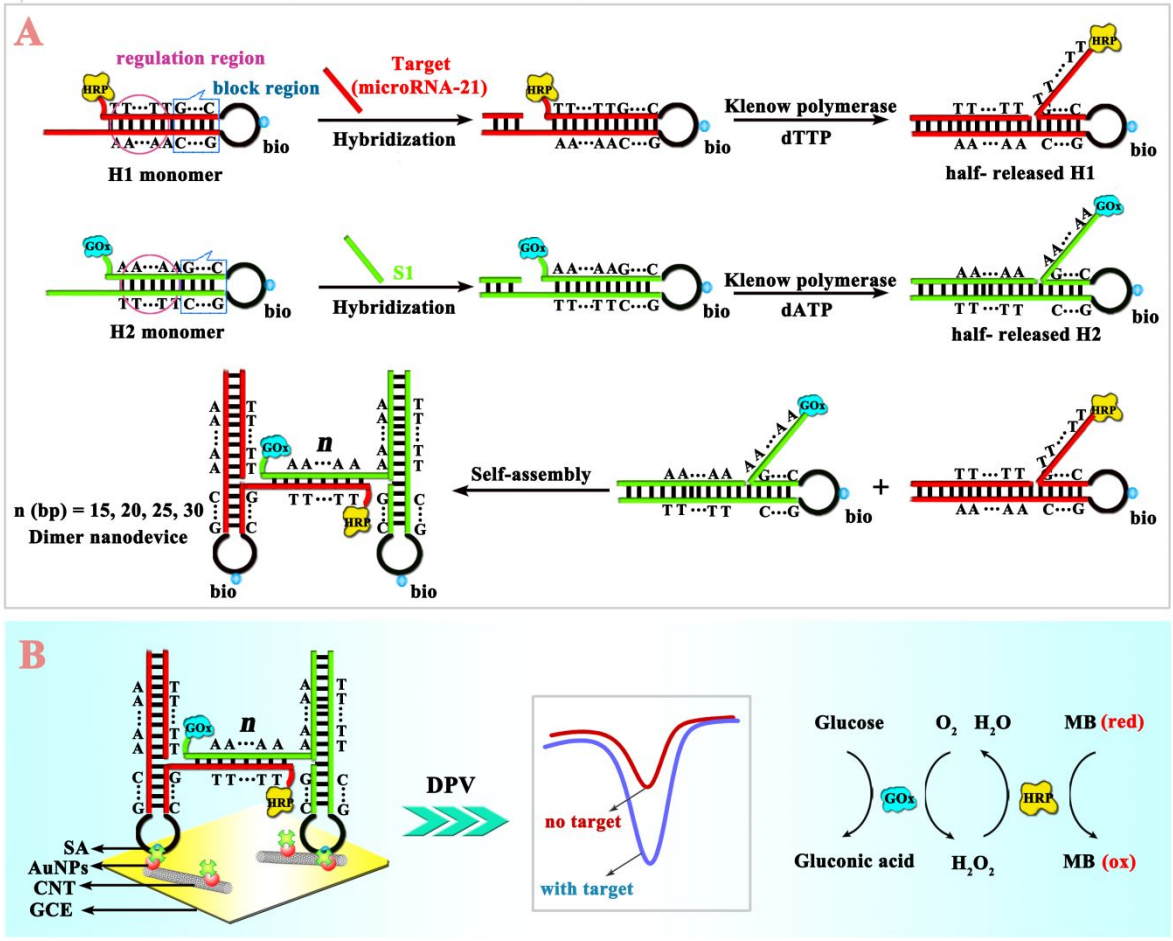

Scheme 1. Schematic Diagrams of (A) target-induced auto-terminated DNA polymerization reaction on two different hairpin DNA monomers (H1, H2) and the preparation of a DNA dimer nanodevice for arranging cascade enzymes; (B) target-induced high efficient enzyme cascade electrocatalysis for electrochemical biosensor construction.

Experimental Section

Materials and Reagents

Glucose oxidase (GOx), N-succinimidyl-3-(2-pyridyldithiol) propionate (SPDP), dithiothreitol (DTT), gold chloride ($HAuCl_4$, 99%), Horseradish peroxidase (HRP), multiwalled carbon nanotubes (MWCNTs, >95% purity), streptavidin (SA), Methylene blue (MB), glucose, $K_3[Fe(CN)_6]$, $K_4[Fe(CN)_6]$ and sodium borohydride ($NaBH_4$) were provide by Shanghai Aladdin Industrial Corporation (Shanghai, China). Klenow polymerase, dATP and dTTP was supplied by New England Biolabs (Beijing, China). All microRNA and DNA oligonucleotides, purified by high-performance liquid chromatograph, were obtained from Sangon Biological Engineering Technology (Shanghai, China). All sequences and modifications of these nucleic acids were displayed in Supporting Information (Table S1).

Apparatus and Measurements

All electrochemical related measurements were performed on a CHI 660E electrochemical workstation (Shanghai Chenhua Instrument, China). DPV measurements parameters were listed as follows: potential range from -0.5 to -0.1 V with 4 mV step potential and 50 mV amplitude. Scanning electron microscopy (SEM, S-4800, Hitachi, Japan) were used for characterizing prepared nanomaterials. Polyacrylamide gel electrophoresis (PAGE) experiments were performed by Bio-Rad imaging system. UV-vis absorption spectrums were obtained by UV-vis spectrophotometer (Shimadzu, Tokyo, Japan).

Preparation of DNA Dimer Nanodevice

In order to prepare the dimer nanodevice, two types of enzyme decorated DNA monomers (HRP-H1, GOx-H2) were first prepared according to our previous method.[32] Then target microRNA-21 and assistant DNA S1 were hybridized with HRP-H1 and GOx-H2, respectively, to form microRNA-21-HRP-H1 complex and S1-GOx-H2 complex. Thereafter, dTTP and klenow polymerase were subjected into microRNA-21-HRP-H1 complex and mixture was incubated at 37°C for 1 h to obtain polymerization product 1 (half-released H1). Meanwhile, dATP and klenow polymerase mixed with S1-GOx-H2 complex and mixture also was incubated at 37°C for 1 h to get polymerization product 2 (half-released H2). Finally, polymerization product 1 and polymerization product 2 were mixed and incubated for 2 h to prepare DNA dimer nanodevice.

Preparation of MWCNTs@AuNPs Nanocomposites

MWCNTs@AuNPs nanocomposites were synthesized according to $NaBH_4$ reduction method with little modification[33,34]. First, $HAuCl_4$ (100 μL, 1%) was dropped into 400 μL MWCNTs solution, and the mixture was stirred for 0.5 h. Next, 50 μL of fresh $NaBH_4$ solution (0.1 M) was introduced and the mixture was stirred vigorously for another 0.5 h. After centrifuging and rinsing by water, obtained precipitate (MWCNTs@AuNPs) was collected for subsequent usage.

Fabrication of the Modified Electrode

Firstly, the bare glassy carbon electrode (GCE, Φ = 4 mm) was polished with alumina slurry and sonicated. After that, 15 μL MWCNTs@AuNPs nanocomposites were dropped on the cleaned electrode and dried at 37°C. Next, 20 μL streptavidin (SA) was added to the modified electrode and

incubated overnight at 4°C. To block the possible remaining adsorption sites, the prepared electrode was then treated with BSA solution (15 μL, 1%) for about 40 min. Finally, 20 μL of DNA dimer product was introduced onto electrode and incubated for 1 h at 37°C. After cleaning, the finished electrode was used for measurements.

Gel Electrophoresis Experiment

Preparation of DNA dimer nanodevice was verified by 16% polyacrylamide gel electrophoresis. After reaction sample mixing with loading buffer was subjected to the gel electrophoresis, the electrophoresis ran at a constant voltage of 120 V for 1.5 h.

Kinetic Measurement

GOx/HRP, glucose and TMB were mixed to perform kinetic experiment. UV-vis spectra were collected to get related Michaelis constants based on followed equation: $1/V = K_m/V_{max}(1/[S] + 1/K_m)$, in which V, K_m, [S] and V_{max} was initial reaction rate, Michaelis-Menten constant, substrate concentration and maximal rate, respectively.

Results and Discussion

Characterization of MWCNTs@AuNPs

The morphologies of the as-prepared MWCNTs and MWCNTs@AuNPs were studied by SEM. In Figure 1A, typical SEM image of MWCNTs displayed a well-dispersed tubular structure. A large number of conductive particles were adsorbed onto MWCNTs, which displayed good dispersion and uniform spherical shape (Figure 1B), proving that AuNPs had been successfully generated on MWCNTs.

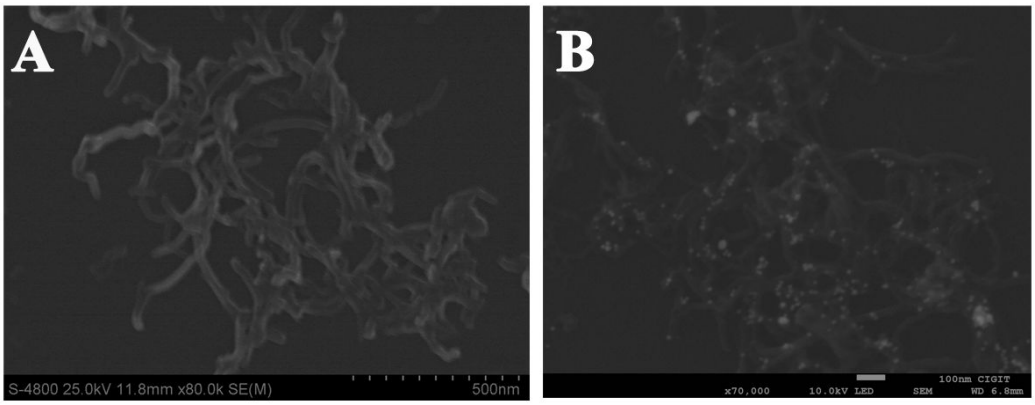

Figure 1. SEM images of (A) MWCNTs and (B) MWCNTs@AuNPs nanocomposites.

PAGE Analysis

The assembly of DNA dimer nanodevice was characterized by PAGE experiment. From Figure 2, lane 1, lane 2 represented the DNA monomers of H1 and H2, respectively. After target microRNA-21 and assistant DNA S1 incubating with H1 and H2, respectively, their products (lane 3, 4) migrated slower than corresponding DNA monomers, which demonstrated the formation of microRNA-21-H1 and S1-H2 complex. Following that, DNA polymerase and corresponding specific dATP or dTTP were introduced to initiate auto-terminated DNA polymerization reactions on H1 and H2. Then two types of polymerization products were mixed and incubated, and the final assembled product in lane 5 showed the slowest migration rate, thus we could infer the successful preparation of designed DNA dimer nanodevice.

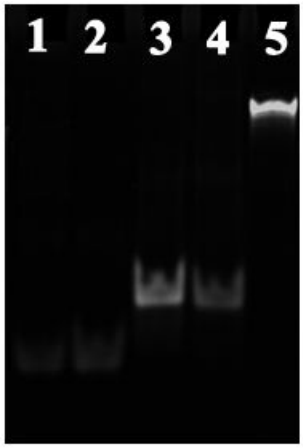

Figure 2. PAGE characterization for the assembly of DNA dimer nanodevice.

Comparison of Different Enzyme Cascade System

In order to verify the highly efficient catalysis of cascade enzymes manipulated by DNA dimer nanodevice on electrode surface, we conducted corresponding comparative experiments and the results were shown in Figure 3. First, when proposed GCE was only modified with MWCNTs@AuNPs, a weak electrochemical signal (Figure 3a) was obtained. Next, enzyme-modified DNA monomers including HRP-H1 and GOx-H2 were randomly immobilized on modified electrode surface, an enhancement in electrochemical response (Figure 3b) was measured. We could deduce that enzyme cascade reaction had happened and facilitated the oxidation of MB electron mediator in measurement solution. Furthermore, after target microRNA-21 inducing the co-assembly of cascade enzymes on dimer nanodevice, the highest electrochemical response (Figure 3c) was monitored, suggesting that the co-assembly of cascade enzymes on dimer nanodevice significantly improved enzyme cascade catalytic efficiency.

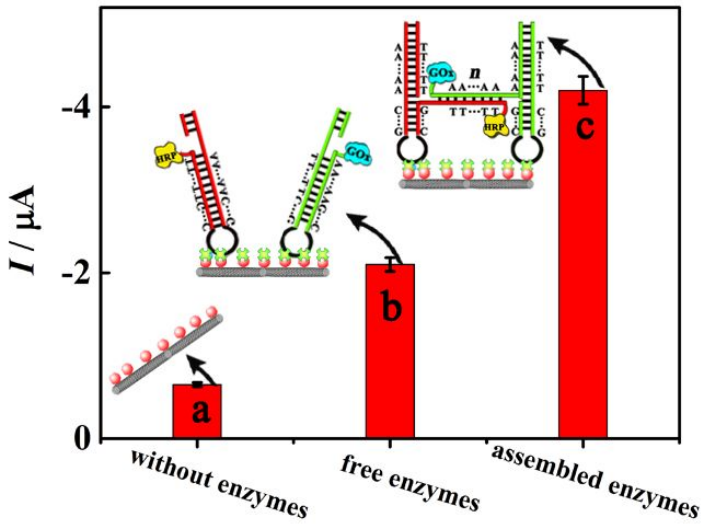

Figure 3. Different DPV signals in varied detection conditions. (a) MWCNTs@AuNPs complex modified on electrode surface without any enzymes immobilization; (b) GOx-H2 and HRP-H1 randomly immobilized on MWCNTs@AuNPs/GCE; (c) Dimer nanodevice manipulated GOx and HRP on MWCNTs@AuNPs/GCE in 2 mL PBS (pH 7.4) buffer possessing 4 μM MB and 5 mM glucose.

Real-Time Absorbance Measurements of Different Cascade Enzyme Systems

The GOx/HRP enzyme cascade reaction began with the GOx catalytic oxidation of glucose, accompanied by the generation of H_2O_2, and then HRP utilized it to oxidize TMB into blue-colored oxidation product with characteristic absorbance at 652 nm[35]. In order to investigate the catalytic efficiency of various cascade enzymes reaction systems, the real-time absorbance measurements were recorded. As shown in Figure 4, blank control sample (only TMB and glucose regent in detection buffer) showed no change in time-dependent absorbance (curve a). After enzyme-modified DNA monomers including GOx-H2 and HRP-H1 were randomly introduced into above detection buffer (free cascade enzyme system), obvious increment of absorbance at 650 nm was measured (curve b), which demonstrated the occur of enzyme cascade reaction. Furthermore, when target

initiated the co-assembly of cascade enzymes on DNA dimer nanodevice, a maximum absorbance change was observed (curve c), implying this system shown the highest cascade catalytic efficiency.

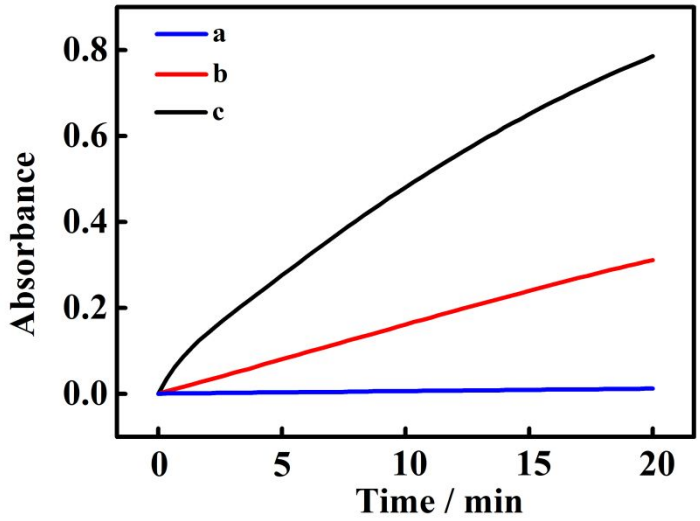

Figure 4. Absorbance-time curves of varied enzyme cascade systems, blank samples (curve a), free cascade enzymes (curve b) and dimer nanodevice manipulated cascade enzymes (curve c) when 1 mM TMB as chromogenic agent.

Kinetic Analysis

To further demonstrate the highly efficient catalysis of dimer nanodevice manipulated cascade enzyme system, the Michaelis-Menten model was used to study their kinetic parameters. K_m (Michaelis constant) and k_{cat} (catalytic rate constant) had been calculated based on the Lineweaver-Burk strategy. As shown in Figure 5, the K_m value of cascade enzymes system manipulated by dimer nanodevice was 1.65 mM (curve b), which was smaller than that of free cascade enzyme system (3.3 mM, curve a). We concluded that dimer nanodevice manipulated cascade enzymes system had a stronger affinity toward substrate than free cascade enzymes. Additionally, the k_{cat}/K_m value for dimer nanodevice manipulated cascade enzymes was calculated to be 5.02 s^{-1} mM^{-1}, and it was 2.6 times higher in comparison with that of free cascade enzymes

system (1.93 s^{-1} mM^{-1}), indicating a higher catalytic efficiency.

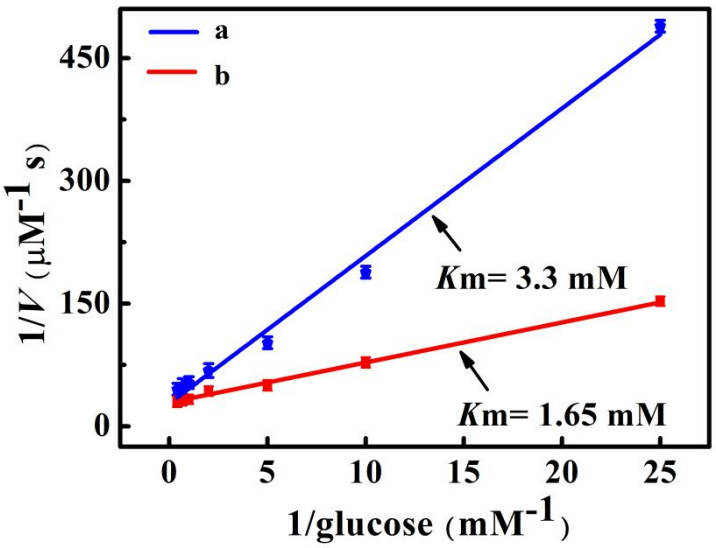

Figure 5. Lineweaver-Burk plots of free cascade enzymes system (curve a) and dimer nanodevice manipulated cascade enzymes systems (curve b) when fixing TMB concentration of 1 mM and varying the glucose concentrations.

Influence of Varied Distances between GOx/HRP on Cascade Reaction

In order to prove that the catalytic effect of enzyme cascade reaction depended on the distance between cascade enzymes of HRP and GOx, the spacer length of rigid dsDNA linker on DNA dimer nanodevice was changed to systematically regulate interenzyme distance. The result was shown in Figure 6, with increasing the spacer length from 15 to 25 bp, the electrochemical response increased continually due to the avoidance of crowding effect[36,37]. Furthermore, with increasing the spacer length from 25 to 30 bp, slight decrease of electrochemical response was measured because of the invalid diffusion effect of reaction intermediate of H_2O_2[38,39]. Thus, the spacer length with 25 bp on DNA dimer nanodevice was chosen as the most favorable distance.

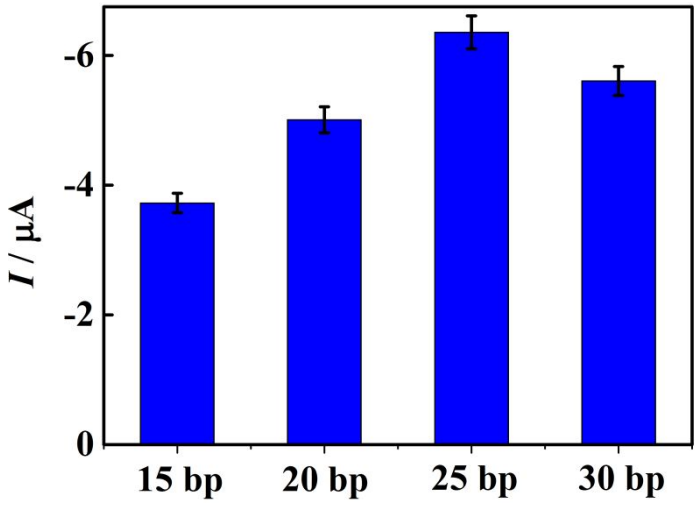

Figure 6. Variation of cascade catalytic response caused by the varied spacer length between cascade enzymes on dimer nanodevice.

Optimization of the Experimental Condition

In this work, excellent electrochemical signal was from enzyme cascade amplification strategy. GOx catalyzed glucose into gluconic acid and got H_2O_2. H_2O_2 served as HRP substrate was then reduced into H_2O, accompanying with MB oxidation for amplified electrochemical response. Thus, MB concentration and glucose concentration could affect the analytical performance of proposed biosensor. In Figure 7A, the MB concentration from 1 to 5 μM had been chosen to test the performance of proposed biosensor and the electrochemical response increased continually accompanied with the increased MB concentration until a plateau was reached at 4 μM. So, 4 μM was employed as the optimal MB concentration. Additionally, glucose with varied concentrations in detection buffer PBS solution (pH 7.0) also was measured. It could be clearly seen from Figure 7B that electrochemical response of proposed biosensor varied with the changeable glucose concentration from 1 to 6 mM, and the response value almost reached to the maximum at 5 mM. Thus, 5 mM was optimal glucose concentration.

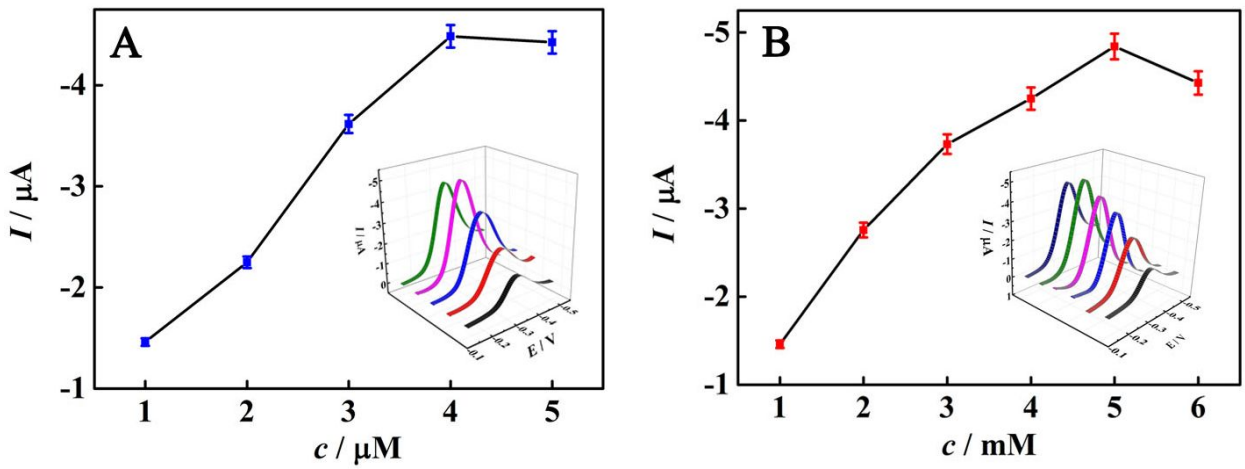

Figure 7. The effect of MB concentration (A) and glucose concentration (B) on current response.

Analytical Performance of Developed Biosensing Platform

To investigate the analytical performance of biosensor, DPV responses with different concentration of microRNA-21 were recorded under the optimal experimental conditions. From Figure 8A, the electrochemical response signal increased accompanied with incremental target concentrations in the range from 0.1 pM to 1 nM. It also could be noted that the calibration plot exhibited a satisfied linear relationship between the electrochemical response and the target microRNA-21 concentration (Figure 8B). The corresponding linear equation is I = -1.212 lg c – 18.281 (r = -0.9965) with a detection limit of 0.03 pM. Moreover, compared with other reported methods (Table 1), the proposed biosensor showed good performance for the microRNA-21 determination, which could be attributed to the fact that target-induced co-assembly of cascade enzymes on a DNA dimer nanodevice with significant enhancement in cascade catalytic efficiency than free cascade enzymes.

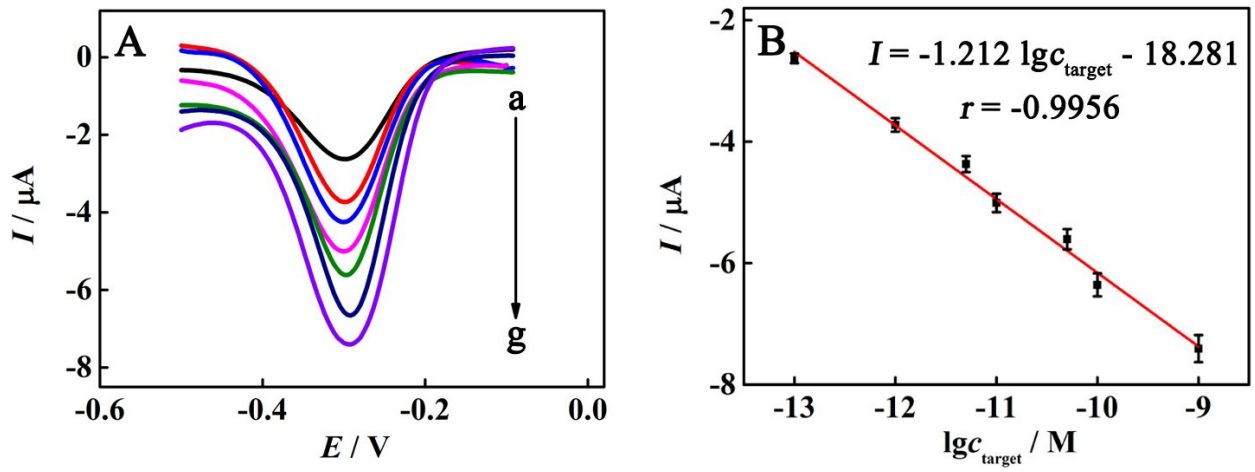

Figure 8. (A) DPV signals of proposed biosensor for the target microRNA-21 at different concentrations with various concentrations of from 0.1 pM to 1 nM. (B) Linear relationship of DPV responses versus the logarithm of microRNA-21 concentration. The error bars stand for the standard deviation of 3 measurements.

Table 1 Comparison of Sensing Performances of Various Methods for microRNA-21 Detection.

Analytical method	Detection limit	Linear range	Ref.
Photoelectrochemistry	0.31 pM	1 pM-100 nM	40
Fluorescence	0.3 pM	1 pM-10 nM	41
Raman Scattering	485 pM	0.5 nM-5 nM	42
Photoluminescence	2.8 pM	5 pM-300 pM	43
Electrochemistry	0.04 nM	0.14 nM-10 nM	44
Electrochemistry	10 pM	100 pM-1 μM	45
Electrochemistry	0.03 pM	0.1 pM-1 nM	This work

Selectivity and Stability of the Fabricated Biosensor

To investigate the selectivity of the biosensor, microRNA-141, microRNA-155 and microRNA let-7a were chosen as interfering substances. Meanwhile, the mixture sample including target and all interfering substances also was tested. As seen in Figure S2, despite the introduction of 10 nM interference substance, no evident electrochemical response change in comparison with that of blank

sample. However, a significant electrochemical response was obtained upon introducing 0.1 nM target microRNA-21, which indicated the high selectivity of developed biosensor. To further study the stability of proposed biosensor, the biosensor was stored at 4°C and intermittently measured every 5 days. After 20 days, there was no obvious change in current response and the response was 90.7% of its initial response, demonstrating great performance of biosensor in stability.

Conclusion

Here, a novel DNA dimer nanodevice was used to regulate the distance between HRP and GOx for high enzyme cascade catalysis for construction of biosensor. In comparison with other scaffolds, the proposed DNA dimer nanodevice avoided the problems of poor biocompatibility and controllability from previous scleroid scaffolds, meanwhile exhibited obvious advantages in terms of assembly yield than previous complicated DNA scaffolds. Consequently, a sensitive electrochemical biosensor for microRNA-21 assay was constructed by utilizing the simple DNA dimer nanodevice to manipulate enzyme cascade reaction, which also provided an alternative way for sensitive detection of other biomolecules in the fields of biosensing and disease diagnosis.

ASSOCIATED CONTENT

Supporting Information. Experimental details for the oligonucleotides sequences used in this work (Table S1), Stepwise Characterization of the Modified Electrode (Figure S1), Application of Proposed Biosensor (Table S2). The Supporting Information is available free of charge on the ACS Publications website.

AUTHOR INFORMATION

* Corresponding authors:

Tel.: +86-23-68252277; Fax: +86-23-68253172.

E-mail address: y198688@swu.edu.cn (Y. L. Yuan), yuanruo@swu.edu.cn (R. Yuan)

NOTES

The authors declare no competing financial interests.

ACKNOWLEDGEMENTS

This work was supported by the National Natural Science Foundation of China (21974108, 21775124 and 21675129), the Fundamental Research Funds for the Central Universities (SWU115037, XDJK2020TY002), the Natural Science Foundation Project of CQ CSTC (cstc2016jcyjA0189).

References

(1) Krall, A. S.; Christofk, H. R. *Nature* **2017**, *546*, 357-358.

(2) Kim, T. H.; Mehrabi, P.; Ren, Z.; Sljoka, A.; Ing, C.; Bezginov, A.; Ye, L. B.; Pomes, R.; Prosser, R. S.; Pai, E. F. *Science* **2017**, *355*, 2355.

(3) Chiang, C. W.; Liu, X. Y.; Sun, J. W.; Guo, J. W.; Tao, L.; Gao, W. P. *Nano Lett*. **2020**, *20*, 1383-1387.

(4) Kuchler, A.; Yoshimoto, M.; Luginbuhl, S.; Mavelli, F.; Walde, P. *Nat. Nanotechnol*. **2016**, *11*, 409-420.

(5) Zhang, Y. F.; Hess, H. *ACS Catal*. **2017**, *7*, 6018-6027.

(6) Fu, J. L.; Yang, Y. R.; Johnson-Buck, A.; Liu, M. H; Liu, Y.; Walter, N. G.; Woodbury, N. W.; Yan, H. *Nat. Nanotechnol*. **2014**, *9*, 531-536.

(7) Wheeldon, I.; Minteer, S. D.; Banta, S.; Barton, S. C.; Atanassov, P.; Sigman, M. *Nat. Chem*. **2016**, *8*, 299-309.

(8) Sun, L. L.; Gao, Y. J.; Xu, Y.; Chao, J.; Liu, H. J.; Wang, L. H.; Li, D.; Fan, C. H. *J. Am. Chem.*

Soc. **2017**, *139*, 17525-17532.

(9) Zhao, X.; Palacci, H.; Yadav, V.; Spiering, M. M.; Gilson, M. K.; Butler, P. J.; Hess, H.; Benkovic, S. J.; Sen, A. *Nat. Chem*. **2018**, *10*, 311-317.

(10) Tsitkov, S.; Hess, H. *ACS Catal*. **2019**, *9*, 2432-2439.

(11) Wheeldon, I.; Minteer, S. D.; Banta, S.; Barton, S. C.; Atanassov, P.; Sigman. M. *Nat. Chem*. **2016**, *8*, 299-309.

(12) Dueber, J. E.; Wu, G. C.; Malmirchegini, G. R.; Moon, T. S.; Petzold, C. J.; Ullal, A. V.; Prather, K. L. J.; Keasling, J. D. *Nat. Biotechnol*. **2009**, *27*, 753-759.

(13) Conrado, R. J.; Wu, G. C.; Boock, J. T.; Xu, H.; Chen, S. Y.; Lebar, T.; Turnsek, J.; Tomsic, N.; Avbelj, M.; Gaber, R.; Koprivnjak, T.; Mori, J.; Glavnik, V.; Vovk, I.; Bencina, M.; Hodnik, V.; Anderluh, G.; Dueber, J. E.; Jerala, R.; DeLisa, M. P. *Nucleic Acids Res*. **2012**, *40*, 1879-1889.

(14) Chado, G. R.; Stoykovich, M. P.; Kaar, J. L. *ACS Catal*. **2016**, *6*, 5161-5169.

(15) Moehlenbrock, M. J.; Toby, T. K.; Waheed, A.; Minteer, S. D. *J. Am. Chem. Soc*. **2010**, *132*, 6288-6289.

(16) Chen, W. H.; Vazquez-Gonzalez, M.; Zoabi, A.; Abu-Reziq, R.; Willner, I. *Nat. Catal*. **2018**, *1*, 689-695.

(17) Ye, J. J.; Chu, T. S.; Chu, J. L.; Gao, B. B.; He, B. F. *ACS Sustainable Chem. Eng*. **2019**, *7*, 18048-18054.

(18) Lian, X. Z.; Chen, Y. P.; Liu, T. F.; Zhou, H. C. *Chem. Sci*. **2016**, *7*, 6969-6973.

(19) Vogele, K.; List, J.; Simmel, F. C.; Pirzer, T. *Langmuir* **2018**, *34*, 14780-14786.

(20) Wang, X. L.; Li, Z.; Shi, J.; Wu, H.; Jiang, Z.; Zhang, W.; Song, X.; Ai, Q. *ACS Catal*. **2014**, *4*, 962-972.

(21) He, L.; Lu, D. Q.; Liang, H.; Xie, S. T.; Luo, C.; Hu, M. M.; Xu, L. J.; Zhang, X. B.; Tan, W. H.

ACS Nano **2017**, *11*, 4060-4066.

(22) Wu, Z.; Liu, G. Q.; Yang, X. L.; Jiang, J. H. *J. Am. Chem. Soc*. **2015**, *137*, 6829-6836.

(23) Hu, Juan.; Liu, M. H.; Zhang, C. Y. *ACS Nano* **2019**, *13*, 7191-7201.

(24) Hou, T.; Xu, N. N.; Wang, W. X.; Ge, L.; Li, F. *Anal. Chem*. **2018**, *90*, 9591-9597.

(25) Chen, Y. H.; Ke, G. L.; Ma, Y. L.; Zhu, Z.; Liu, M. H.; Liu, Y.; Yan, H.; Yang, C. J. *J. Am. Chem. Soc*. **2018**, *140*, 8990-8996.

(26) Fu, J. L.; Liu, M. H.; Liu, Y.; Woodbury, N. W. Yan, H. *J. Am. Chem. Soc*. **2012**, *134*, 5516-5519.

(27) Ke, G. L.; Liu, M. H.; Jiang, S. X.; Qi, X. D.; Yang, Y. R.; Wootten, S.; Zhang, F.; Zhu, Z.; Liu, Y.; Yang, C. J.; Yan, H. *Angew. Chem. Int. Ed*. **2016**, *55*, 7483-7486.

(28) Wang, D.; Chai, Y. Q.; Yuan, Y. L.; Yuan, R. *Anal. Chem*. **2019**, *91*, 3561-3566.

(29) Zhou, L.; Liu, Y.; Shi, H.; Yang, X. H.; Huang, J.; Liu, S. Y.; Chen, Q. S.; Liu, J. B. Wang, K. M. *ChemBioChem*. **2018**, *19*, 2099-2106.

(30) Liu, M. H.; Fu, J. L.; Hejesen, C.; Yang, Y. H.; Woodbury, N. W.; Gothelf, K.; Liu, Y.; Yan, H. *Nat. Commun*. **2013**, *4*, 2127.

(31) Kou, B. B.; Chai, Y. Q.; Yuan, Y. L.; Yuan, R. *Anal. Chem*. **2018**, *90*, 10701-10706.

(32) Wang, D.; Chai, Y. Q.; Yuan, Y. L.; Yuan, R. *Anal. Chem*. **2019**, *91*, 3561-3566.

(33) Dou, B. T.; Li, J.; Jiang, B. Y.; Yuan, R.; Xiang, Y. *Anal. Chem*. **2019**, *91*, 2273-2278.

(34) Zhuang, J. Y.; Lai, W. Q.; Xu, M. D.; Zhou, Q.; Tang, D. P. *ACS Appl. Mater. Interfaces* **2015**, *7*, 8330-8338.

(35) Liu, Y.; Zheng, Y. L.; Chen, Z.; Qin, Y. L.; Guo, R. *Small* **2019**, *15*, 1804987.

(36) Zhang, Y. F.; Hess, H. *ACS Catal*. **2017**, *7*, 6018-6027.

(37) Wang, D.; Chai, Y. Q.; Yuan, Y. L.; Yuan, R. *Anal. Chem*. **2019**, *91*, 3561-3566

(38) Fu, J. L.; Liu, M. H.; Liu, Y.; Woodbury, N. W.; Yan, H. *J. Am. Chem. Soc*. **2012**, *134*, 5516-5519.

(39) Kong, L. Q.; Wang, D.; Chai, Y. Q.; Yuan, Y. L.; Yuan, R. *Anal. Chem*. **2019**, *91*, 10289-10294.

(40) Chu, Y.; Wu, R.; Fan, G. C.; Deng, A. P.; Zhu, J. J. *ACS Sustainable Chem. Eng*. **2018**, *6*, 11633-11641.

(41) Xi, Q.; Zhou, D. M.; Kan, Y. Y.; Ge, J.; Wu, Z. K.; Yu, R. Q.; Jiang, J. H. *Anal. Chem*. **2014**, *86*, 1361-1365.

(42) Alessandro, C.; Chiara, N.; Andrea, L.; Francesco, G.; Fabrizio, G.; Paola, R. *Anal. Chem*. **2016**, *88*, 9554-9563.

(43) Guo, J. J.; Mingoes, C.; Qiu, X.; Hildebrandt N. *Anal. Chem*. **2019**, *91*, 3101-3109.

(44) Campuzano, S.; Torrente-Rodriguez, R. M.; Lopez-Hernandez, E.; Conzuelo, F.; Granados, R.; Sanchez-Puelles, J. M.; Pingarron, J. M. *Angew. Chem. Int. Ed*. **2014**, *53*, 6168-6171.

(45) Liu, S. P.; Su, W. Q.; Li, Z. L.; Ding, X. T. *Biosens. Bioelectron*. **2015**, *71*, 57-61.

For TOC Only

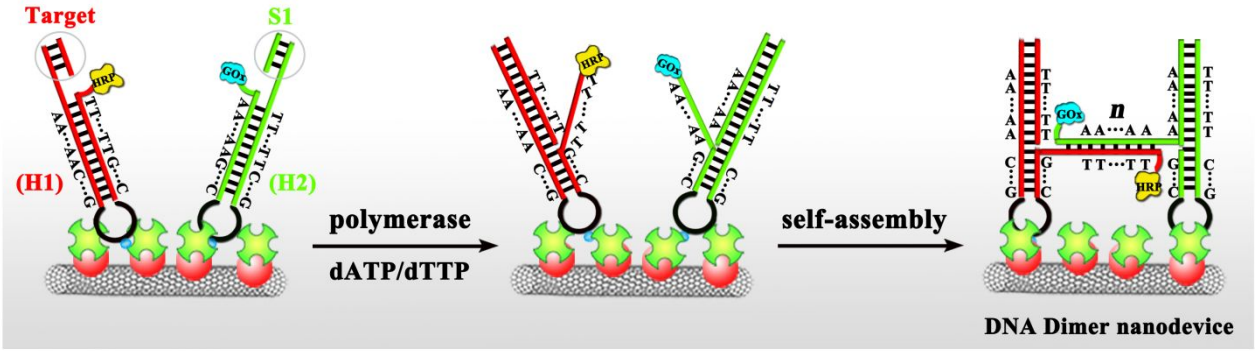
Target
S1
(H1)
(H2)
polymerase
dATP/dTTP
self-assembly
DNA Dimer nanodevice